International Journal of Applied Engineering Research ISSN 0973-4562 Volume 10, Number 24 (2015) pp 44341-44346

A Multiband CMOS RF Power Amplifier with Double Secondary Transformer Matching

Veeraiyah Thangasamy, Noor Ain Kamsani, Mohd Nizar Hamidon, Shaiful Jahari Hashim

Faculty of Engineering, Universiti Putra Malaysia, 43400, UPM Serdang, Malaysia
nkamsani@upm.edu.my

Muhammad Faiz Bukhori

Faculty of Engineering & Built Environment, Universiti Kebangsaan Malaysia, 43600, UKM Bangi, Malaysia

Zubaida Yusoff

Faculty of Engineering, Multimedia University, 63100, Cyberjaya, Malaysia

Vinesh Thiruchelvam

School of Engineering, Asia Pacific University of Technology and Innovation, 57000, Kuala Lumpur, Malaysia

Abstract
With increasing consumer demand for wireless devices to support multiple air standards and applications, there have been increased trends for the implementation multiband (MB) power amplifier (PA) for wireless handsets. This paper presents a novel design of an MB PA based on an industry-standard 130nm process technology. PAs using conventional transformer based matching has a narrow bandwidth. Hence, a PA using cascode differential architecture with novel single primary and double secondary transformer matching is proposed in this design. The proposed PA has wider 3dB bandwidth from 1GHz-2.3GHz covering 11 LTE FDD frequency bands. The PA has 22.5dB gain with peak output power of 28.4dBm. The PA is operated in class-AB linear mode; and PAE of 37% at 1-dB compression point and 65% at peak output power is achieved. The achieved ACPR is-42.6dBc which is well confined within the modern LTE linearity specifications.

Keywords: Multiband, Power Amplifier, Transformer Matching, Power Added Efficiency (PAE), Long Term Evolution (LTE).

Introduction

3GPP 4G LTE is a driving force in the mobile communication industry[1][2]. Smartphones used nowadays have increasing demand for high data rate services such as: social networking, web browsing, video streaming, music downloads, gaming, and many other popular applications. As such, the wireless communication devices are facing the challenge of supporting multiple air interface technologies such as GSM, HSPA, HSPA+, WCDMA and LTE (multimode). Additionally, with the growing number of frequency bands used in different geographies around the world and to facilitate international roaming, these devices are required to operate on a number of frequency bands (multiband)[3]. Thus, the market for RF front-end components is growing rapidly driven by adoption of multimode, multiband handsets[4].

Fig. 1 shows the block diagram of smartphone transceiver based on discrete architecture[3]. It has separate signal path one for each band; requiring high BOM count, large area and consumes more power. The 4G and next-generation networks (NGN) needs to have converged architecture as shown in Fig.1(b); and thus requiring less BOM count, smaller area and lesser power consumption. Thus, in the converged architecture the RF power amplifier is required to operate on multiple frequency bands in order to support different networks/applications.

Number of multiband PAs presented in the literature has limited bandwidth range of operation. For example, the PA presented by Kang *et.al*[5] is using InGaP/GaAs HBT process that operates in 820MHz-920MHz bandwidth; the dual-mode PA presented by Cho *et.al*[6] using InGaP/GaAs HBT operates in the 1.7GHz-2.0GHz bandwidth; and GaN HEMT based MB PA presented by Kim *et.al*[7] operates in the 1.8GHz-2.3GHz band.

Applications on CMOS process have been reported on multiband PAs integrated circuit design in the literature. For example, a switching mode PA by Aref *et.al*[8] presented in the 90nm TSMC CMOS technology operates with 1.6GHz-2.6GHz bandwidth. Another PA presented by Kim *et.al*[9] was designed using 130nm CMOS process which covers the frequency range 1.6GHz-1.9GHz. To support multiband operation, the PA is required to have a wider bandwidth in the LTE spectrum. Though number of applications is reported in the literature in the LTE bandwidth spectrum, their bandwidth of operation is not sufficient to cover the multiband requirement of RF front-ends. This is more evident when a transformer is used for matching it results in a narrow bandwidth; which includes the PA design in [9]-[12]

In this work, we propose a novel single primary and double secondary transformer for matching. The use of transformer with proposed double secondary structure in this design has two parameters enhancement. Firstly, the bandwidth of the PA has increased, making the PA design more suitable for the multiband requirement of emerging smartphones and next generation (NGN) applications. Secondly, the efficiency of the PA has been increased. Compared with PA manufactured with other process technology, the proposed MB PA in cost-effective CMOS process will provide a greater integration possibility with other blocks in a mobile device.

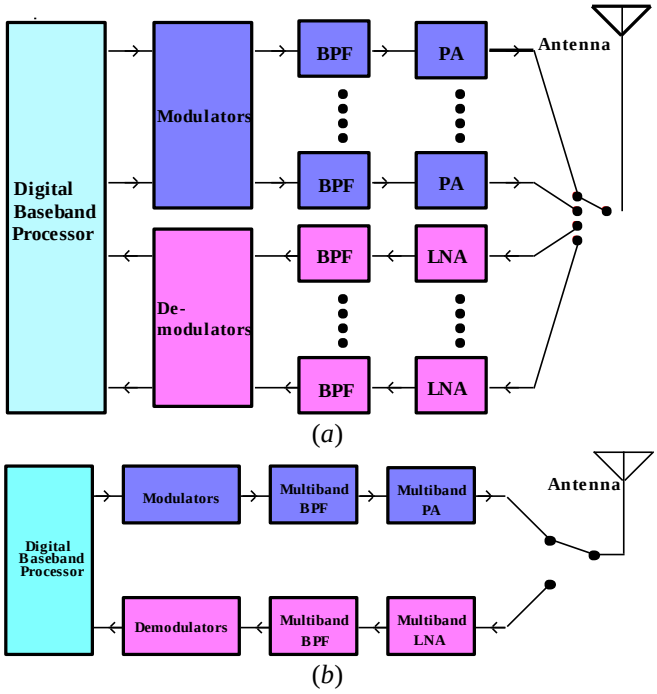

Fig. 1. Smartphone block diagram (*a*) based on discrete architecture (*b*) based on converged architecture

Proposed Multiband PA Design

Cascoded differential amplifier architecture is chosen in the design of PA core as it offers many advantages than the common source amplifier. The output power from a single common source amplifier is proportional to the square of the supply voltage as given by Eqn. (1).

$$P_{o,single} = \frac{V_{DD}^{2}}{2R} \qquad 1$$

Eqn. (1) reveals that to obtain high output power, it needs to increase the supply voltage. Therefore, a differential architecture is preferred in this work as it doubles the voltage swing at the drain terminal of the transistor, which in turn quadruples the output power without increasing the supply voltage value as in Eqn.(2).

$$P_{o,differential} = \frac{(2V_{DD})^{2}}{2R} = 4P_{o,single} \qquad 2$$

In Silterra (Silterra, Kulim, Kedah, Malaysia) 130nm CMOS PDK, there are two types of transistors. The first type is thin oxide transistor that has a nominal supply voltage of 1.2V and the second type is thick oxide transistor that has the nominal supply voltage of 2.5V. When either one of these transistors is designed as common source amplifier, the supply voltage is too low to produce higher output power for the power amplifier for LTE/WCDM standards. Hence, in order to achieve the required output power, cascode configuration is chosen in this design. For this cascode differential amplifier design, supply voltage of 3.3V is chosen to conform to wireless handsets battery standards. The cascoded configuration can also protect the transistor from higher stress, which could lead to gate oxide breakdown. Thick oxide transistor with a higher breakdown voltage of 15.4V is used in the cascode stage, and thin oxide transistor with a low breakdown voltage of 6.8V is used in the transconductance stage. Thus, the design benefits are high gain from the thin oxide transistor and high voltage swing from the thick oxide transistor.

The single primary double secondary transformer used for impedance matching is shown in Fig. 2(a) and its symbol shown in Fig. 2(b). The RF transformer windings are designed in the top metal layer which is 3.3µm thick. The underpass interconnects are drawn using the immediate next layer (Metal 7). The width of primary and secondary windings is 30µm each, and the spacing is 5µm. The use of transformer as a matching device has several advantages, which are: 1) removal of DC blocking capacitors and RF chokes 2) relatively lower insertion loss compared to L, T, Π type matching networks 3) easy second-harmonic filtering through the center taps of the transformer, and 4) differential-to-single ended conversion capabilities needed to drive the load.

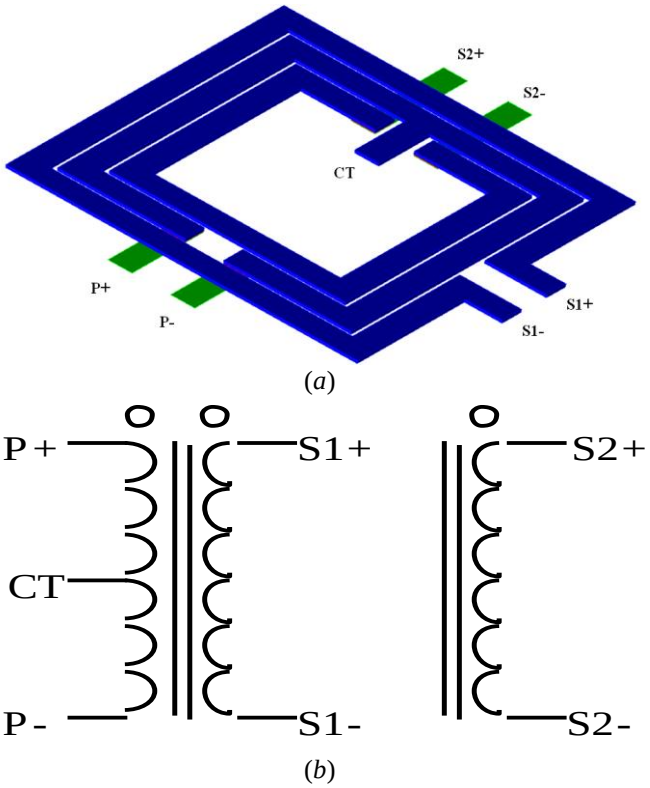

Fig. 2. Proposed single primary double secondary transformer (a) layout (b) symbol with terminal identification

Electromagnetic simulation was performed for the design of transformer using the Momentum tool of Advanced Design System (ADS, Keysight EEsof EDA, Santa Rosa, CA, USA) and the parameters extracted was imported as Touchstone file to the Cadence (Cadence Design System, San Jose, CA, USA) to perform the simulation. Transformer parameters were calculated from the S-parameters using the Eqn. (3) through (7) [13].

$$L_P = imag(Z(1,1))/\omega \quad (3)$$

$$L_S = imag(Z(2,2))/\omega \quad (4)$$

$$Q_P = imag(Z(1,1))/real(Z(1,1)) \quad (5)$$

$$Q_S = imag(Z(2,2))/real(Z(2,2)) \quad (6)$$

$$k = \sqrt{\frac{((Y(1,1))^{-1} - Z(1,1)) \cdot Z(2,2)}{imag(Z(1,1)) \cdot imag(Z(2,2))}} \quad (7)$$

Fig. 3 shows the complete schematic of the proposed multiband PA with the double secondary transformer. When a transformer with single primary and single secondary is used for matching, then secondary inductor of the transformer will be tuned by using a parallel capacitor for the center frequency of the desired channel, and it will result in a narrow bandwidth. In the proposed transformer there are two secondaries; energy is transferred from the primary into both the secondaries by means of mutual coupling. Both the secondaries are tuned by using parallel capacitors for two different frequencies in the desired frequency bandwidth range as given by Eqn. (8) and (9).

$$f_{C,S1} = \frac{1}{2\pi\sqrt{L_{S1}C_{S1}}} \quad (8)$$

$$f_{C,S2} = \frac{1}{2\pi\sqrt{L_{S2}C_{S2}}} \quad (9)$$

where $f_{C,S1}$ and $f_{C,S2}$ are the resonant frequency of the secondary tuned circuits and these two frequencies should fall within the desired bandwidth of the PA and should be at equidistant from the center frequency of the band to get flat pass band response

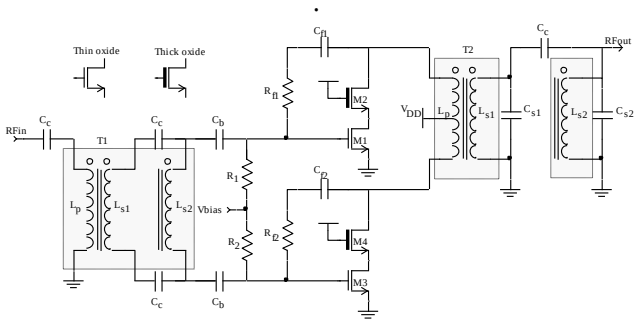

Fig. 3. Schematic diagram of the proposed MB PA using double secondary matching transformer.

In the proposed circuit, the input transformer is also a single primary and double secondary transformer. However, it is not resonant-tuned because: 1) resonant-tuning lowers the bandwidth; 2) resonant-tuning increases the input drive of the amplifier which affects the linearity. Modern PAs requires high linearity[14] because of the high PAPR associated with varying envelope modulation; and hence the designed PA is operated in class-AB mode by means of external bias voltage (V_{bias}) applied via R_1 and R_2. R_{f1}-C_{f1} and R_{f2}-C_{f2} provides feedback necessary for stable operation of the PA. M1 and M3 are thin oxide transistors; M2 and M4 are thick oxide transistor. For V_{DD}=3.3V, the drain of M2 and M4 swings up to twice the V_{DD}, that is for 6.6V and hence thick oxide transistor with higher gate-drain breakdown voltage is chosen for the common gate cascode transistor. Capacitor C_b provides necessary blocking for the DC bias from entering into transformer secondaries. Coupling capacitor C_c helps for AC signal coupling between the transformer secondaries. The component values of the designed MB PA are shown in Table 1.

Table 1. Component values of the designed MB PA

Components	Value
M1, M3	W=2×64×10µm, L=130nm
M2,M4	W=3×64×10µm, L=280nm
C_c, C_b	100fF, 30pF
C_f, R_f	2pF, 700Ω
R_1, R_2	100kΩ, 100kΩ
C_{s1}, C_{s2}	2pF, 100fF
Transformer T1, T2	Size: 900µm×900µm Layer width: 30µm Spacing: 5µm Thickness: 3.3µm

Proposed Multiband PA Simulation Results

The proposed design of multiband PA was simulated using Cadence Spectre® in the 130nm CMOS process from Silterra PDK. The obtained S-parameters are shown in Fig.4; which has the gain of 22.5dB with bandwidth from 1GHz-2.3GHz. It can be seen two peaks in the S22 response which are due the double secondary tuned circuits, and that had increased the 3dB bandwidth of the PA. This wide bandwidth obtained can cover 11 FDD LTE bands: band 1, 2, 3, 4, 9, 10, 11, 21, 23, 24 and 25. The obtained S11 and S22 are nearly-5dB and-9dB respectively making the PA well matched to the source and the load.

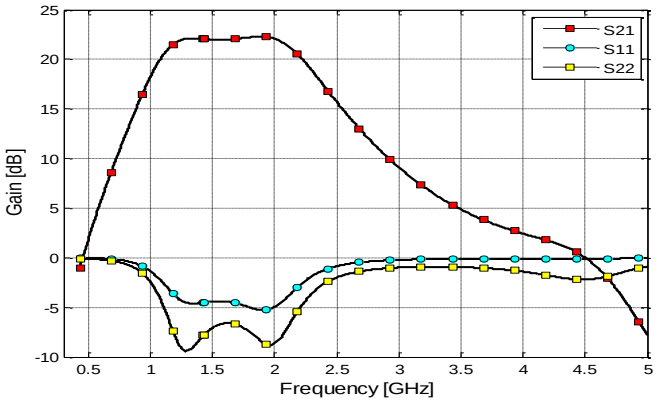

Fig. 4. S-parameters (S21, S11, S22) of the proposed MB PA

The PA output power versus input power is shown in Fig. 5. It was obtained from the periodic steady state analysis at 1900MHz. The response is linear with power at 1-dB compression point as 23dBm and saturated power as 28.4dBm. Power amplifier for LTE application requires only 23dBm output power; thus making this design fulfills LTE class-3 power output specification.

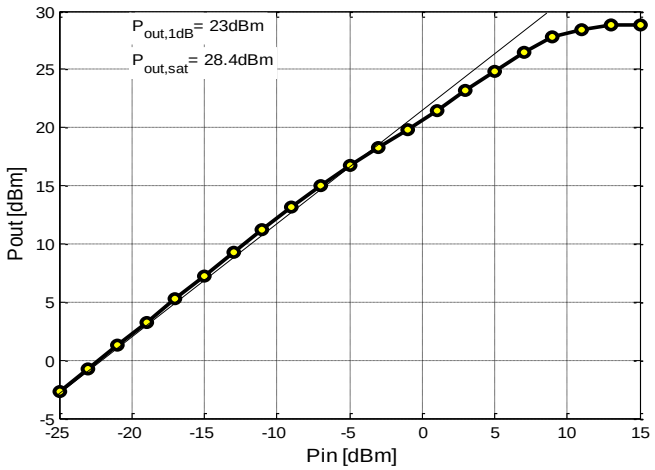

Fig. 5. Power output versus power input of the proposed MB PA at 1900 MHz

The obtained PAE versus output power of the PA is plotted in Fig. 6. PAE of 37% at 1-dB point and 65% at peak output power is achieved. Double secondary transformer matching is one of the reasons for this high PAE attainment even without any efficiency enhancement techniques applied. The third-order intercept point (IP3) calculation is depicted in Fig. 7. For this, two signals at same power level but with slightly different frequency: 1901MHz and 1900MHz were applied to the PA and periodic ac analysis was carried out and an IP3 of 9dBm is obtained. From the results, the third-order harmonic distortion (THD) of-25dBc is obtained at the 1-dB point.

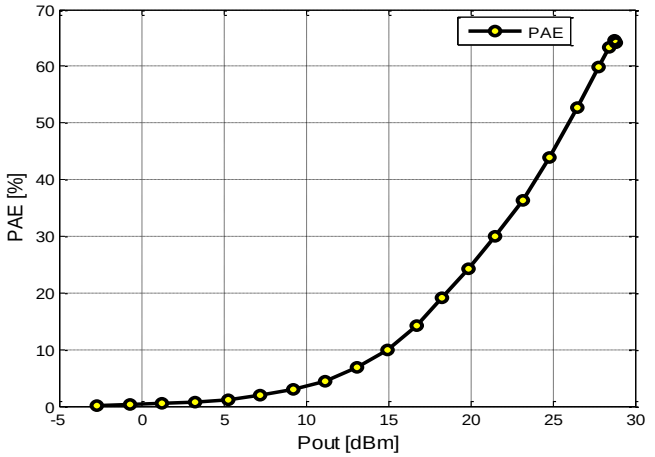

Fig. 6. PAE versus power output of the proposed MB PA at 1900MHz

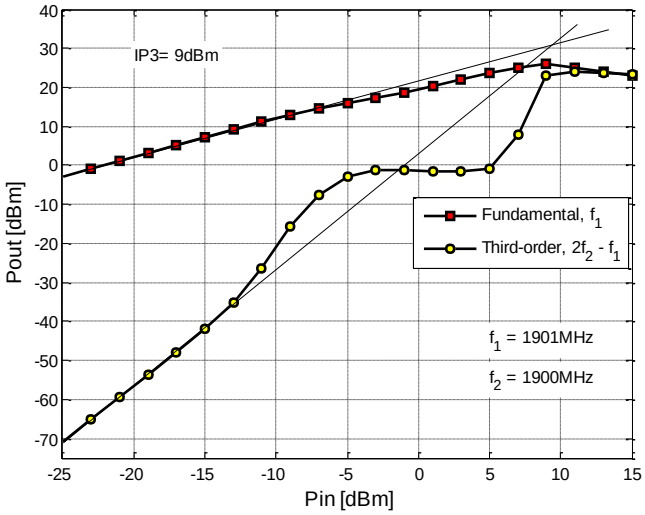

Fig. 7. Third-order intercept point (IP3) of the proposed MB PA

Stability factor of the PA is also an important parameter to ensure that the PA never undergoes any unwanted oscillation. The stability factor graphs obtained over the bandwidth range of operation is shown in Fig. 8. It shows that the stability factors B_{1f} is less than 1 and K_f is greater than 1 through the entire bandwidth; thus confirming the PA operation is well stable. Fig. 9 shows the power spectral density of the proposed MB PA for CDMA carrier applied at output power of 23dBm. The ACPR of-42.6dBc is obtained for adjacent channel and-55.9dBc obtained for alternate channel which are well below the specification.

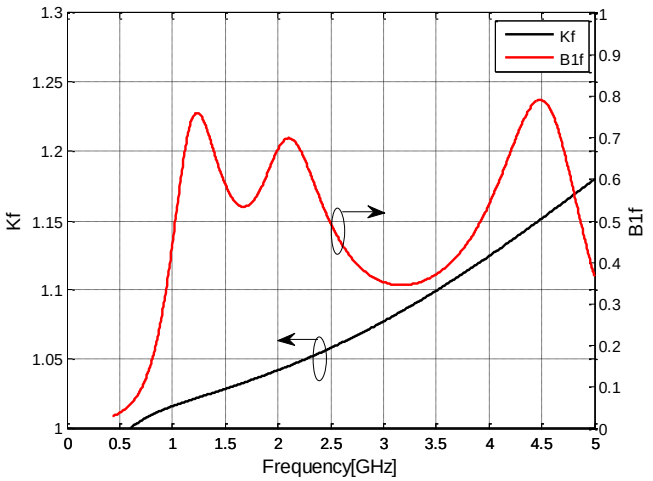

Fig. 8. Stability factors (Kf, B1f) versus frequency of the proposed MB PA

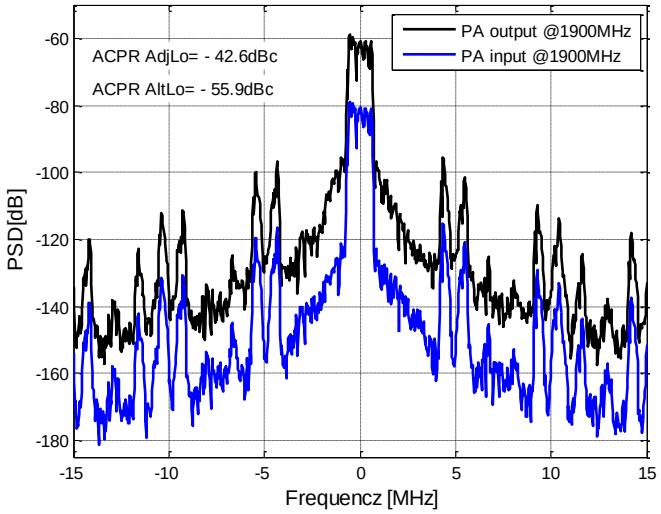

Fig. 9. Power Spectral Density (PSD) of the proposed MB PA

Table 2. Comparison of the proposed MB PA with state-of-the-art CMOS MB PA

Comparison	This work	[8]	[9]	[10]	[11]	[12]
Bandwidth	1.0-2.3 GHz	1.6-2.6 GHz	1.6-1.9GHz	1.9GHz-2.6GHz	1.8GHz-2.2GHz	1.67-1.97GHz
Matching Network	On-chip double secondary transformer	Off-chip Load Transformation Network	On-chip single secondary transformer	On-chip single secondary transformer	On-chip single secondary transformer	On-chip single secondary transformer
Process	130nm CMOS	90nm CMOS	130nm CMOS	90nm CMOS	130nm CMOS	180nm CMOS
Supply [V]	3.3	2.8	3.4	3.3	3.3	3.4
Operation	Class AB	Class F	Class AB	Class AB	Class AB	Class AB
Psat [dBm]	28.4	27	32	30.1	17	30.5
Gain [dB]	22.5	22.1	22	28	13.2	23.7
Peak PAE [%]	65	43	45	33	21	42
EET*	no	yes	yes	no	no	no
ACPR [dBc]	-42.6 (Adj Ch) -55.9 (Alt Ch)	Complies with GSM mask	Complies with EDGE mask	Complies with WiMax mask	n/a	-35

Table 2 summarizes the performance of the proposed multiband PA with the state-of-the-art MB CMOS PAs. The proposed double secondary transformer matching based PA in the CMOS process has better performance than the other PA with single secondary transformer matching employed. Especially, nearly a 2 to 4 fold increment in the bandwidth is obtained thus coving more number of LTE bands. Also the PAE is increased considerably because the proposed double secondary transformer couples more energy from primary into secondary than the single secondary transformer does. Thus the proposed MB PA design in the cost-effective CMOS process when integrated in the transceiver module will prove to be small size and possess high integration capability with other blocks in the transceiver.

Conclusion

A MB PA with novel double secondary transformer based matching has been proposed in view of obtaining wide bandwidth that can support for 11 LTE bands for smartphones and next generation wireless devices. The double secondary transformer at the output of the PA is resonant-tuned for two different frequencies to achieve wide bandwidth than a single secondary transformer. The design employed cascode differential architecture and it exhibits higher PAE and higher output power with single stage PA. The obtained ACPR results for modern linearity are well within the specification. The proposed MB CMOS PA offers greater solution for next generation wireless handsets by providing small form factor, low cost and high integration capability with other digital signal processor in the wireless RF front-ends.

Acknowledgements

This work was supported by Universiti Putra Malaysia Research University Grant Scheme (RUGS)

References

[1] Y. Li, R. Zhu, D. Prikhodko, and Y. Tkachenko, “LTE power amplifier module design: Challenges and trends,” in IEEE International Conference on Solid-State and Integrated Circuit Technology, 2010, pp. 192-195.

[2] V. Mangayarkarasi, D. R. S. Sudeepa, R. Hema, and N. R. Raajan, “Performance estimation of BER in LTE system,” Int. J. Appl. Eng. Res., vol. 9, no. 9, pp. 1025-1034, 2014.

[3] N. Cheng and J. P. Young, “Challenges and Requirements of Multimode Multiband Power Amplifiers for Mobile Applications,” in IEEE Compound Semiconductor Integrated Circuit Symposium, 2011, pp. 1-4.

[4] N. Q. Bolton, “Mobile Device RF Front-End TAM Analysis and Forecast,” in CS MANTECH Conference, 2011, pp. 39-42.

[5] S. Kang, U. Kim, Y. Kwon, and J. Kim, “A Multi-mode Multi-band Reconfigurable Power Amplifier for Low Band GSM/UMTS Handset Applications,” in IEEE Topical Conference on Power Amplifiers for Wireless and Radio Applications, 2013, pp. 16-18.

[6] Y. Cho, D. Kang, J. Kim, D. Kim, B. Park, and B. Kim, “A Dual Power-Mode Multi-Band Power Amplifier With Envelope Tracking for Handset Applications,” IEEE Trans. Microw. Theory Tech., vol. 61, no. 4, pp. 1608-1619, Apr. 2013.

[7] J. Kim, F. Mkadem, and S. Boumaiza, “A High Efficiency and Multi-Band / Multi-Mode Power Amplifier using a Distributed Second Harmonic Termination,” in European Microwave Conference, 2010, pp. 1662-1665.

[8] A. F. Aref and R. Negra, “A Fully Integrated Adaptive Multiband Multimode Switching-Mode CMOS Power Amplifier,” IEEE Trans. Microw. Theory Tech., vol. 60, no. 8, pp. 2549-2561, Aug. 2012.

[9] H. Kim, Y. Yoon, O. Lee, K. An, D. Lee, W. Kim, C. Lee, and J. Laskar, “A Fully Integrated CMOS RF Power Amplifier with Tunable Matching

Network for GSM/EDGE Dual-Mode Application," in IEEE MTT-S International Microwave Symposium, 2010, pp. 800-803.

[10] D. Chowdhury, C. D. Hull, O. B. Degani, Y. Wang, and A. M. Niknejad, "A Fully Integrated Dual-Mode Highly Linear 2.4GHz CMOS Power Amplifier for 4G WiMax Applications," IEEE J. Solid-State Circuits, vol. 44, no. 12, pp. 3393-3402, Dec. 2009.

[11] J. Fu, N. Mei, Y. Huang, and Z. Hong, "CMOS high linearity PA driver with an on-chip transformer for W-CDMA application," J. Semicond., vol. 32, no. 9, pp. 095006-6, Sep. 2011.

[12] B. Koo, T. Joo, Y. Na, and S. Hong, "A Fully Integrated Dual-Mode CMOS Power Amplifier for WCDMA Applications," in IEEE International Solid-State Circuits Conference, 2012, pp. 82-84.

[13] Q. El-Gharniti, E. Kerhervé, and J. B. Bégueret, "Modeling and characterization of on-chip transformers for silicon RFIC," IEEE Trans. Microw. Theory Tech., vol. 55, no. 4, pp. 607-615, 2007.

[14] V. Thangasamy, N. Ain Kamsani, M. Hamidon, and M. Faiz Bukhori, "An overview of RF power amplifier techniques and effect of transistor scaling on its design parameters," Int. J. Appl. Eng. Res., vol. 9, no. 2, pp. 257-276, 2014.